Strategic Network Utilization in a Wireless Structural Control System for Seismically Excited Structures

R. Andrew Swartz, M.ASCE[1]; and Jerome P. Lynch, M.ASCE[2]

Abstract: The benefits associated with structural control include the mitigation of undesired structural responses and reduction in the probability of damage to structural components during seismic events. Structural control systems in current use depend on extensive wired communication systems to connect sensors and actuators with a centralized controller. While wired architectures are appropriate when control systems are small, the cost and installation complexity of tethered systems increases as the control system grows large (i.e., defined by hundreds of nodes). Alternatively, wireless sensors are proposed for use in large-scale structural control systems to keep costs low and to improve system scalability. Wireless sensors are capable of collecting state data from sensors, communicating data between themselves, calculating control actions, and commanding actuators in a control system. However, bandwidth and range limitations of the wireless communication channel render traditional centralized control solutions impractical for the wireless setting. While computational abilities embedded with each wireless sensor permit fully decentralized control architectures to be implemented, strategic utilization of the wireless channel can improve the performance of the wireless control system. Toward this end, this paper presents a partially decentralized linear quadratic regulation control scheme that employs redundant state estimation as a means of minimizing the need for the communication of state data between sensors. The method is validated using numerical simulations of a seismically excited six-story building model with ideal actuators. Additional experimental validation is conducted using a full-scale physical realization of the six-story building. A wireless sensor network commanding magnetorheological dampers is shown to be effective in controlling a multistory structure using the partially decentralized control architecture proposed.

DOI: 10.1061/(ASCE)ST.1943-541X.0000002

CE Database subject headings: Sensors; Structural control; Estimation; Seismic effects; Networks.

Introduction

While it has been shown that structural control systems can be effective in mitigating the dynamic response of large-scale structures (Soong 1990; Housner et al. 1997; Spencer and Nagarajaiah 2003), system costs and long-term reliability concerns still remain as barriers to widespread adoption of such systems. Semiactive structural control devices have recently been developed to address these cost and reliability concerns. Compared to large active actuators, semiactive structural control devices such as magnetrorheological (MR) dampers (Dyke et al. 1998; Hatada et al. 2000; Gavin et al. 2001), electrorheological (ER) dampers (McMahon and Makris 1997), variable-orifice dampers (Kurino et al. 2003), and variable-stiffness devices (Nagarajaiah and Mate 1998) are relatively inexpensive to design and fabricate, require little power, and can be powered from battery power supplies (Kurata et al. 1999).

Semiactive control systems have been successfully deployed in numerous structural applications (Spencer and Nagarajaiah 2003; Kajima-Corporation 2006). The forces achievable with these semiactive devices are smaller in magnitude than those achievable by an active device (e.g., active mass damper). However, a highly effective control system can be produced when a large number of semiactive devices are installed in a single structure. Recently completed structures employing semiactive control technology include the 54-story Mori Tower employing 356 semiactive hydraulic dampers (SHD), the 38-story Nihonbashi Mitsui Tower employing 96 SHD, and the Shiodome Tower, employing 88 SHD, all located in Tokyo (Kajima-Corporation 2006). As the number of control devices increases, the vulnerability of the control system as an entity to the failure of a single control device is reduced.

Use of semiactive control devices in a centralized control system may not be a complete solution to the aforementioned cost and reliability problems often associated with structural control. While semiactive devices are less costly than active actuators, as the number of control devices grows, the cost savings realized by use of semiactive devices quickly erodes due to the high cost of the extensive wiring needed between sensors, actuators, and controllers. Additionally, centralized computation of command forces requires a central computer to collect data, calculate control forces, and command actuators in a short time frame; these calculations get more difficult to complete in the allocated time as the system grows. One solution to these two problems is achieved in Kajima Corporation's HiDAX system which is a fully decentralized control system; SHD devices are distributed throughout a structure to independently provide control forces between consecutive floors (Kajima-Corporation 2006). No communication is offered between SHD devices with each device calculating a con-

[1]Ph.D. Candidate, Dept. of Civil and Environment Engineering, Univ. of Michigan, Ann Arbor, MI 48109-2125.

[2]Assistant Professor, Dept. of Civil and Environment Engineering, Univ. of Michigan, Ann Arbor, MI 48109-2125 (corresponding author). E-mail: jerlynch@umich.edu

Note. Discussion open until October 1, 2009. Separate discussions must be submitted for individual papers. The manuscript for this paper was submitted for review and possible publication on March 31, 2008; approved on October 21, 2008. This paper is part of the ***Journal of Structural Engineering***, Vol. 135, No. 5, May 1, 2009. ©ASCE, ISSN 0733-9445/2009/5-597–608/$25.00.

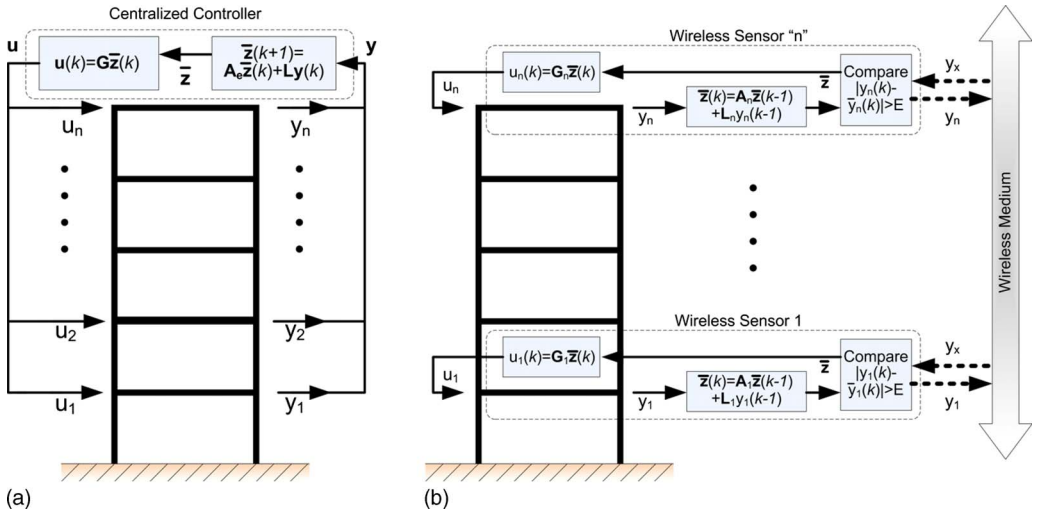

Fig. 1. (a) Classical centralized controller approach to structural control; (b) proposed distributed control system assembled from network of wireless sensors serving as controllers

trol action based solely on its collocated sensor output. The actions of these controllers are derived globally, but in operation they act independently, not sharing data.

Improving coordination between distributed controllers would obviously improve the results their use yields. Wireless sensors have been successfully employed for monitoring civil structures (Lynch et al. 2004b; Lynch and Loh 2006). Wireless sensors can be installed without the expense of cable installation, providing a low cost link between distributed elements of the monitoring system. Wireless sensors with embedded computational power are able to perform onboard data interrogation, eliminating the need to transmit raw data to centralized servers (Straser and Kiremidjian 1998). Recent work has demonstrated the ability of wireless sensors to act as active sensors (Chintalapudi et al. 2005) and controllers (Kawka and Alleyne 2004). As controllers, wireless sensors are responsible for collecting sensor data, calculating desired control forces, and commanding actuators for centralized (Wang et al. 2006b; Loh et al. 2007) and decentralized (Wang et al. 2006a; Lin et al. 2007; Loh et al. 2007) control architectures.

Wireless control systems have inherent limitations that prevent them from functioning as perfect replacements for cable-based control systems. For example, wireless data transmissions add latency, thereby reducing sampling frequencies and the overall effectiveness of the controller. Another concern is data loss. Self-acknowledging protocols for data transmission (e.g., TCP/IP) guarantee data transmission but also introduce additional delay. Several established transmission protocols used in real-time wireless feedback control, including polling, time division multiple access (TDMA), random access (RA) with and without acknowledgement, and carrier sensing multiple access/collision avoidance (CSMA/CA), have been evaluated (Liu and Goldsmith 2004). Wireless feedback schemes using the IEEE 802.11b protocol are also proposed with sample rate adaptation used to overcome the effects of communication latency (Colandairaj et al. 2007). However, this approach introduces random, lengthy delays into the communications. Network protocols without acknowledgement (e.g., UDP) can eliminate this source of latency entirely, but require a control algorithm that is tolerant of data loss (Ploplys et al. 2004). Another functional constraint of wireless communications is that the available communication bandwidth is fixed (Arms et al. 2004). In large control systems, care must therefore be taken not to exceed the channel capacity. The range of the wireless signal is also limited. Finally, wireless communication is power-intensive. Especially for battery powered wireless sensors, wireless radios have greater power requirements than any other hardware component (Lynch and Loh 2006; Nagayama et al. 2007).

To overcome these wireless sensor limitations, a partially distributed control scheme is proposed that is tolerant of data loss and in which the available wireless bandwidth is strategically leveraged to improve control performance. The proposed system is an adaptation of a partially distributed control scheme developed for networked control by Yook et al. (2002). In it, wireless sensors are responsible both for collecting sensor output and supplying actuator commands based on linear quadratic regulation. In addition, each are embedded with identical estimators, in this case, steady-state Kalman estimators. The resulting state estimates are compared to locally available measured data and used for feedback control force computation when errors between measured and estimated state data are small. Only when the error exceeds a threshold value specified by the designer are the measured values wirelessly transmitted to the network of sensors, allowing other sensors to update their own estimates. Detailed derivation of the method is presented in the following section followed by a review of wireless sensing for civil infrastructure. Then, results from simulations and an experimental study using Narada wireless sensor units to control and actuate MR dampers for seismic disturbance rejection in a six-story building model are presented and discussed.

Redundant Estimator Network Control Architecture

As opposed to traditional centralized systems [Fig. 1(a)] where system outputs are communicated to a single controller for formulation of control actions, a wireless control system is assembled from a network of wireless sensors that serve as a coordinated set of distributed controllers. Each wireless sensor is responsible for measuring system outputs, calculating control actions, and issuing command signals to actuators. The resulting architecture [Fig. 1(b)] differs significantly from the centralized

approach in that: (1) the centralized controller is abandoned for an architecture in which each actuator has its own controller (i.e., a wireless sensor); and (2) the dedicated wired communication system is replaced by a flexible wireless communication channel.

There are challenges associated with real-time control on a wireless network including power consumption (Lynch and Loh 2006) and fixed bandwidth (Arms et al. 2004). One possible approach to addressing these limitations is to fully decentralize the control system by eliminating the communication between controllers. Such an approach has proven effective for semiactive hydraulic dampers deployed in large civil structures (Kurino et al. 2003). However, decentralization does not take advantage of the benefits offered by communication between controllers. Alternatively, a centralized control system can be replicated upon a wireless control system by forcing all wireless sensors to broadcast their measurements at every time step. Unfortunately, this approach places a hefty demand on the available communication bandwidth; hence, the approach is not scalable for large wireless sensor networks. Past work in wireless structural control reveals low-sample rates are required to ensure reliable data delivery when implementing a centralized wireless control system (Lynch et al. 2008).

A partially decentralized distributed control algorithm is proposed to achieve an optimal compromise between the decentralized and centralized control approaches. The benefits associated with data exchange between wireless sensors are preserved, while use of the communication channel is minimized both to keep channel performance high and power demands at the individual sensors low. A redundant estimation framework first proposed by Yook et al. (2002) for networked control systems is adopted. As shown in Fig. 1(b), each wireless sensor employs a Kalman filter to estimate the full state response, $\bar{\mathbf{z}}$, based upon the measured system output, y_i, at the sensor's degree of freedom. If the control system is decentralized, the state estimate would be used to calculate the control action, u_i. In contrast, the redundant estimation framework proposed herein compares the estimated, $\bar{y}$, and measured output, y, to quantify the error inherent in the estimator. If the estimated state variable at the ith measurement degree of freedom is inaccurate, then the estimators executed at the other degrees of freedom (that are derived from the same model) will also have inaccurate estimates of the ith degree of freedom's state variables. If the error is above a threshold, the ith wireless sensor broadcasts the measured state variables. Upon receipt of the true measured output from the ith degree of freedom, the other wireless sensors update their estimated states before calculating the control force to be applied. In essence, wireless bandwidth is strategically leveraged to improve decentralized control performance as is described in the following sections.

State-Space System Model

The base-excited structural system is modeled in continuous time as an n-degree-of-freedom (DOF) linear time-invariant, lumped mass shear structure whose equation of motion is

$$\mathbf{M}\ddot{\mathbf{x}}(t) + \mathbf{C_d}\dot{\mathbf{x}}(t) + \mathbf{K}\mathbf{x}(t) = -\mathbf{M}\ell\ddot{x}_g(t) + \mathbf{L}\mathbf{u}(t) \tag{1}$$

with $\mathbf{M}$, $\mathbf{C_d}$, and $\mathbf{K} \in \mathbf{R}^{n\times n}$ corresponding to the mass, damping, and stiffness matrices, respectively. The displacement vector relative to the base of the structure is $\mathbf{x} \in \mathbf{R}^{n\times 1}$, ground displacement is x_g, and $\ell \in \mathbf{R}^{n\times 1}$ is a vector in which each term is unitary. If control forces, $\mathbf{u} \in \mathbf{R}^{m\times 1}$, are applied to the system then the actuator locations are described by the location matrix, $\mathbf{L} \in \mathbf{R}^{n\times m}$. The variable t represents continuous time.

The equation of dynamic equilibrium described by Eq. (1) can be reformulated in state space as

$$\dot{\mathbf{z}}(t) = \mathbf{A}\mathbf{z}(t) + \mathbf{B}\mathbf{u}(t) + \mathbf{E}\ddot{x}_g(t) \tag{2}$$

where the state is $\mathbf{z}^T = \{\mathbf{x}^T \dot{\mathbf{x}}^T\} \in \mathbf{R}^{2n\times 1}$ and

$$\mathbf{A} = \begin{bmatrix} \mathbf{0} & \mathbf{I} \\ -\mathbf{M}^{-1}\mathbf{K} & -\mathbf{M}^{-1}\mathbf{C_d} \end{bmatrix} \in \mathbf{R}^{2n\times 2n}$$

$$\mathbf{B} = \begin{bmatrix} \mathbf{0} \\ \mathbf{M}^{-1}\mathbf{L} \end{bmatrix} \in \mathbf{R}^{2n\times m}, \quad \mathbf{E} = \begin{bmatrix} \mathbf{0} \\ -\ell \end{bmatrix} \in \mathbf{R}^{2n\times 1}$$

With sensors installed in the structure, the measurable system output, $\mathbf{y} \in \mathbf{R}^{p\times 1}$, is represented by a linear sum of the state of the system and the applied control forces

$$\mathbf{y}(t) = \mathbf{C}\mathbf{z}(t) + \mathbf{D}\mathbf{u}(t) + \mathbf{F}\ddot{x}_g(t) \tag{3}$$

with $\mathbf{C} \in \mathbf{R}^{p\times 2n}$; $\mathbf{D} \in \mathbf{R}^{p\times m}$; and $\mathbf{F} \in \mathbf{R}^{p\times 1}$.

Before a digital control system can be implemented, the continuous-time state-space model [Eq. (2)] is converted into the discrete-time domain with time step T_s using the zero order hold (ZOH) discretization method (Franklin et al. 2002)

$$\mathbf{z}(k+1) = \mathbf{\Phi}\mathbf{z}(k) + \mathbf{\Gamma}\mathbf{u}(k) + \mathbf{\Lambda}\ddot{x}_g(k) \tag{4}$$

where

$$\mathbf{\Phi} = e^{\mathbf{A}T_S} \in \mathbf{R}^{2n\times 2n},$$

$$\mathbf{\Gamma} = \left(\int_0^{T_S} e^{\mathbf{A}\tau} d\tau\right)\mathbf{B} \in \mathbf{R}^{2n\times m}, \quad \mathbf{\Lambda} = \left(\int_0^{T_S} e^{\mathbf{A}\tau} d\tau\right)\mathbf{E} \in \mathbf{R}^{2n\times 1}$$

Optimal Linear Quadratic Regulation (LQR) Control

The LQR control strategy is widely employed in the structural control field because it offers an optimal control solution minimizing the response of the structure, $\mathbf{y}$, while simultaneously minimizing control effort. The LQR control solution determines the optimal control force trajectory, $\mathbf{u}$, by minimizing the scalar cost function, J

$$J(\mathbf{u}) = \sum_{k=1}^{\infty} (\mathbf{z}^T(k)\mathbf{Q}_1\mathbf{z}(k) + \mathbf{u}^T(k)\mathbf{Q}_2\mathbf{u}(k)) \tag{5}$$

where $\mathbf{Q}_1 = \mathbf{C}_{\mathbf{LQR}}^T\mathbf{C}_{\mathbf{LQR}}$ with $\mathbf{C}_{\mathbf{LQR}}$ being a linear mapping between the state and a response to be regulated ($\tilde{\mathbf{y}} = \mathbf{C}_{\mathbf{LQR}}\mathbf{z}$), and $\mathbf{Q}_2 \in \mathbf{R}^{p\times p}$ = symmetric positive definite matrix that weighs the relative importance of control effort against the structure output. The matrices $\mathbf{Q}_1$ and $\mathbf{Q}_2$ are often termed the state cost matrix and input cost matrix, respectively (Franklin et al. 2002).

To ensure the optimal control trajectory is physically feasible, minimization of the LQR cost function is constrained by Eq. (4) through the use of Lagrangian multipliers (Stengle 1994). The full derivation of the LQR control law may be found in any standard control text (Bryson and Ho 1975). The resulting linear control law is

$$\mathbf{u}(k) = [[\mathbf{Q}_2 + \mathbf{\Gamma}^T\mathbf{P}\mathbf{\Gamma}]^{-1}\mathbf{\Gamma}^T\mathbf{P}\mathbf{\Phi}]\mathbf{z}(k) = \mathbf{G}\mathbf{z}(k) \tag{6}$$

with $\mathbf{G} \in \mathbf{R}^{m\times 2n}$, the linear gain matrix, and the Riccati matrix, $\mathbf{P} \in \mathbf{R}^{2n\times 2n}$, derived from the solution to the algebraic Riccati equation

$$\mathbf{P} = \mathbf{\Phi}^T[\mathbf{P} - \mathbf{P}\mathbf{\Gamma}[\mathbf{Q}_2 + \mathbf{\Gamma}^T\mathbf{P}\mathbf{\Gamma}]^{-1}\mathbf{\Gamma}^T\mathbf{P}]\mathbf{\Phi} + \mathbf{Q}_1 \tag{7}$$

Kalman State Estimation

To calculate the optimal control forces using the LQR control law proposed in Eq. (6), the entire state vector, $\mathbf{z}(k)$, is needed at each time step. For most structural control systems, measurement of the complete state of the system is not an economical option. Rather, the measured output of the structure, $\mathbf{y}(k)$, is communicated to a centralized controller where an estimator is implemented for estimation of the state, $\hat{\mathbf{z}}$. Among the many methods available for state estimation, Kalman filtering is the most widely implemented by the structural control community (Soong 1990; Chu et al. 2005).

The Kalman estimator assumes the structure is disturbed at its base by the broad-band excitation, $w(k)$, with a zero mean and covariance of R_w

$$\mathbf{z}(k+1) = \mathbf{\Phi}\mathbf{z}(k) + \mathbf{\Gamma}\mathbf{u}(k) + \mathbf{\Lambda}w(k) \tag{8}$$

Furthermore, the output measurement of the system is corrupted by white noise, $\mathbf{v}(k) \in \mathbf{R}^{p\times 1}$ with covariance, $\mathbf{R}_v \in \mathbf{R}^{p\times p}$

$$\mathbf{y}(k) = \mathbf{C}\mathbf{z}(k) + \mathbf{v}(k) \tag{9}$$

The estimation problem seeks to minimize the state estimation error covariance, $\mathbf{P_e}$

$$\mathbf{P_e} = \lim_{t\to\infty}[(\mathbf{z}-\hat{\mathbf{z}})(\mathbf{z}-\hat{\mathbf{z}})^T] \in \mathbf{R}^{2nx2n} \tag{10}$$

First, given an estimate of the state at the last time step, $\hat{\mathbf{z}}(k-1)$, the state at the current time step can be predicted

$$\bar{\mathbf{z}}(k) = \mathbf{\Phi}\hat{\mathbf{z}}(k-1) + \mathbf{\Gamma}\mathbf{u}(k-1) \tag{11}$$

However, the estimate can be improved by taking into account the measurement error at the current step

$$\hat{\mathbf{z}}(k) = \bar{\mathbf{z}}(k) + \mathbf{L}(k)(\mathbf{y}(k) - \mathbf{C}\bar{\mathbf{z}}(k)) \tag{12}$$

The estimator gain matrix, $\mathbf{L}(k) \in \mathbf{R}^{2n\times p}$, is intended to minimize the error inherent to state estimation by considering the error in the measurement. The estimator gain is time variant but will settle to a steady-state value over the course of the control system execution (Franklin et al. 2002). As a result, the steady-state estimator gain is implemented in most control systems to keep the implementation of the Kalman filter simple. Derivation of the steady-state estimator gain matrix mimics that of the linear quadratic regulator with a nonlinear Riccati equation recursively solved for the steady-state error covariance, $\mathbf{P_e}$.

Redundant Estimation and State Recovery

An independent Kalman estimator is designed for each degree of freedom of the system as shown in Fig. 1(b). To ensure the estimation states are identical across the system, the same model of the system ($\mathbf{\Gamma}$, $\mathbf{\Phi}$, and $\mathbf{\Lambda}$), disturbance covariance, R_w and noise covariance, R_v, are employed in deriving each Kalman estimator. The only difference in the derivations is the output matrix, $\mathbf{C}$, that is uniquely defined for each degree of freedom.

With an estimator embedded in each wireless sensor, the sensors can locally calculate a control force, u, based upon their state estimate, $\bar{\mathbf{z}}$. Should a pure decentralized architecture be adopted, the control system performance would be limited by the quality of the estimator. Hence, the performance of the decentralized control system can be improved if the wireless communication channel is utilized. In the redundant estimator framework, state recovery is proposed as a mechanism by which estimator performance can be improved without placing a hefty burden on the wireless channel (Yook et al. 2002).

State recovery consists of estimators exchanging measurement data when estimation errors are large. Each estimator in the control system compares its locally measured system output, $\mathbf{y}_i$, to that estimated, $\bar{\mathbf{y}}_i$, where

$$\bar{\mathbf{y}}_i(k) = \mathbf{C}_i\bar{\mathbf{z}}(k) \tag{13}$$

The error between the measured and estimated state response is defined as

$$\mathbf{E} = \bar{\mathbf{y}}_i - \mathbf{y}_i \tag{14}$$

where $\mathbf{E} \in \mathbf{R}^{p\times 1}$. Should the error exceed a predefined threshold, then the wireless sensor replaces the estimated state variables with those measured. Additionally, the measurement is transmitted to the wireless sensor network, thus allowing other estimators to "recover" the accurate (i.e., measured) state value. In this manner, state estimates are synchronized throughout the wireless network to be within an allowable error range. State recovery allows a wirelessly networked control system to attain a higher level of performance compared to a purely decentralized system in which controllers do not communicate.

For example, the estimator at the ith degree of freedom makes an estimate based on the measured output of the system

$$\mathbf{y}_i = \begin{Bmatrix} x_i & \dot{x}_i \end{Bmatrix}^T \tag{15}$$

Using this measurement, an estimate for the full state is made using Eqs. (11) and (12). The estimator then compares the estimate $\bar{\mathbf{y}}_\mathbf{i}$, to the measured system output, $\mathbf{y}_i$. If the difference is greater than the established error bound, H

$$\begin{aligned} &\text{Transmit } x_i \quad \text{if } \bar{x}_i - x_i > H_d \\ &\text{Transmit } \dot{x}_i \quad \text{if } \bar{\dot{x}}_i - \dot{x}_i > H_v \end{aligned} \tag{16}$$

After transmission, the updated state vector, $\bar{\mathbf{z}}^*$, at each degree of freedom in the system becomes

$$\bar{\mathbf{z}}^* = \{\bar{x}_1 \cdots \bar{x}_{i-1} \;\; x_i \;\; \bar{x}_{i+1} \cdots \bar{x}_n \;\; \bar{\dot{x}}_1 \cdots \bar{\dot{x}}_{i-1} \;\; \dot{x}_i \;\; \bar{\dot{x}}_{i+1} \cdots \bar{\dot{x}}_n\}^T \tag{17}$$

The calculation of the control force is then $u_i = \mathbf{G}_i\bar{\mathbf{z}}^*$ where $\mathbf{G}_i \in \mathbf{R}^{1\times 2n} = i$th row of the global LQR gain matrix, $\mathbf{G}$.

The difference between the true state response and the updated state estimate can be expressed as

$$\bar{\mathbf{z}}^* = \mathbf{z} + \mathbf{e} \tag{18}$$

where

$$\mathbf{e} = \{e_1 \cdots e_{i-1} \;\; 0 \;\; e_{i+1} \cdots e_n \;\; \dot{e}_1 \cdots \dot{e}_{i-1} \;\; 0 \;\; \dot{e}_{i+1} \cdots \dot{e}_n\}^T \tag{19}$$

Each term of the vector represents the error between the estimated and true state variable; however, if the estimate is updated by the state recovery algorithm, then the corresponding error is zero. Through state recovery, the error inherent to the estimator is bounded by the threshold vector, $\mathbf{H}$. Hence, the calculated control force vector for the global system, $\mathbf{u}$, is

$$\mathbf{u} = \mathbf{G}\bar{\mathbf{z}}^* = \mathbf{G}\mathbf{z} + \mathbf{G}\mathbf{e} \tag{20}$$

In essence, the estimation error amplified by the feedback gain represents a bounded disturbance on the control force with the bound dictated by the thresholds, H, used (Yook et al. 2002).

Wireless Sensing

Due to their relative low cost and ease of installation, wireless sensors are gaining popularity as an alternative to cable-based sensor networks (Lynch and Loh 2006). Successful field deployments in actual civil structures over the past 5 years have demonstrated the feasibility and value of the technology (Lynch et al. 2003; Kurata et al. 2005; Lynch et al. 2006; Whelan et al. 2007; Pakzad et al. 2008). Research continues to advance wireless sensing with distributed computing within the wireless sensing network now emerging as a new usage strategy for the technology. Sensor-centric computing, where wireless sensors process their own measurement data, has been illustrated for modal analysis (Lynch et al. 2004a) and damage detection (Tanner et al. 2002; Clayton et al. 2005; Hou et al. 2005). More recently, network-wide computing architectures have also been proposed for mode shape estimation of civil structures (Zimmerman et al. 2008). Wireless sensors with the ability to affect their surroundings are also suitable for "active" sensing applications (Chintalapudi et al. 2005) thereby eliminating reliance on ambient vibrations for excitation. Once actuation is integrated into the design of a wireless sensor, it becomes possible for wireless sensors to perform feedback control functions as well. In this study, a wireless sensor capable of commanding structural actuators is proposed.

Validation of the state recovery control technique for a seismically excited civil structure is conducted using the "Narada" wireless sensing units developed at the University of Michigan (Swartz et al. 2005). The Narada wireless sensing unit is composed of four primary modules located on a four-layer printed circuit board (PCB): the computational core, the sensing interface, the actuation interface, and the wireless radio. The computational core consists of a low-power, 8-bit, Atmel ATmega128 microcontroller and 128 kB of random access memory. The microcontroller is responsible for automating the operation of the unit and is capable of processing raw sensor data. The additional memory included in the core is for data storage. The sensing interface consists of a four-channel, 16-bit, Texas Instruments ADS8341 analog to digital converter (ADC). The actuation interface is a two-channel, 12-bit, Texas Instruments DAC7612 digital to analog converter (DAC). The wireless radio selected is the Chipcon CC2420 IEEE 802.15.4 Zigbee wireless transceiver. A functional diagram and picture of a Narada unit are presented in Fig. 2, with a summary of the unit's capabilities detailed in Table 1.

For maximum flexibility, a multithreaded operating system (OS) and application software were developed. A fully functional physical (PHY) layer, controlling physical parameters of the radio (channel selection, unit and network identification, and modulation of data on the carrier frequency), and medium access control (MAC) layer, defining timing and access to wireless communications, were written to conform to the IEEE 802.15.4 wireless communication standard. For structural control applications, the IEEE 802.15.4 MAC layer introduces excessive latency, requiring up to 16 ms per data transmission. A simplified, though less adaptable, MAC layer is developed for this study using an unacknowledged TDMA communication scheme to keep data transmission times below 2 ms. In total, the calculations of state vector estimates, determination of control forces, and the transmission of state data (when necessary) occurs within 33 ms. As will be shown, clock drift and jitter during the course of the test occasionally disrupt the TDMA scheme leading to randomly lost packets, most especially when demand for the available bandwidth is high. Finally, taking advantage of the multithreaded OS, the desired control force can be calculated as the unit is in communication with the wireless sensor network. The timing of a typical control step is presented in Fig. 3.

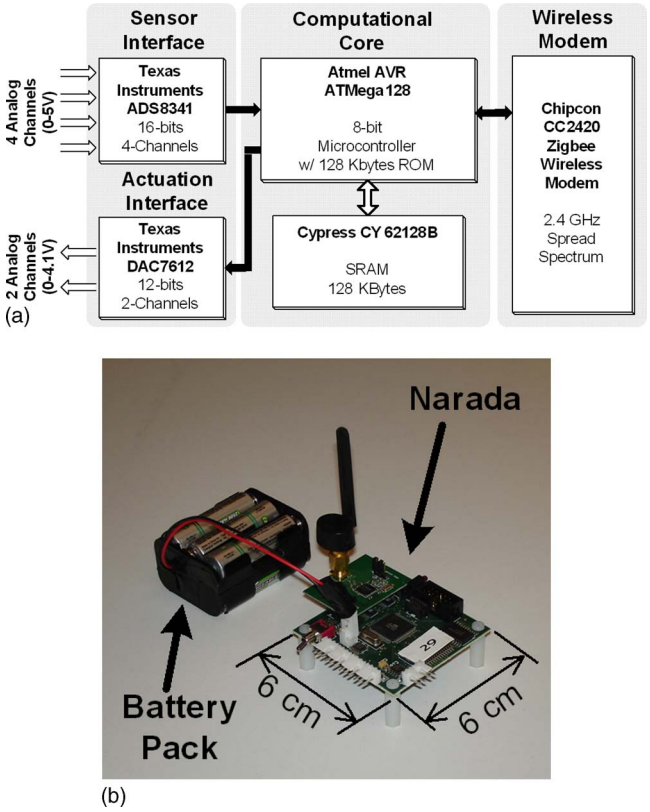

Fig. 2. Narada wireless sensing unit: (a) functional diagram; (b) unit pictured with battery power supply

Verification of Control Strategy

The structure (Fig. 4) that is the subject of both the simulation and experimental phases of this study is a partial scale, single-bay, six-story building. The floor height is 1.0 m per story and the bays are 1.0 m wide by 1.5 m deep. The columns are 15 cm $\times$ 2.5 cm rectangular steel sections oriented in their flexurally

Table 1. Narada Performance Specifications

Narada WSU performance specifications		
Number of sensing channels	4	—
Sensor resolution	16	bits
Analog input range	0–5	V
Maximum sampling rate	10,000	Hz
Number of actuation channels	2	
Actuation interface resolution	12	bits
Analog output range	0–4.1	V
Radio frequency range	2,405–2,480	MHz
Radio transmission rate	250	kbps
Radio transmission range	50	m
Power source	6 AA	NiMH batt.
Power draw: radio off (radio on)	120 (180)	mW
Cost ($)	200	per unit

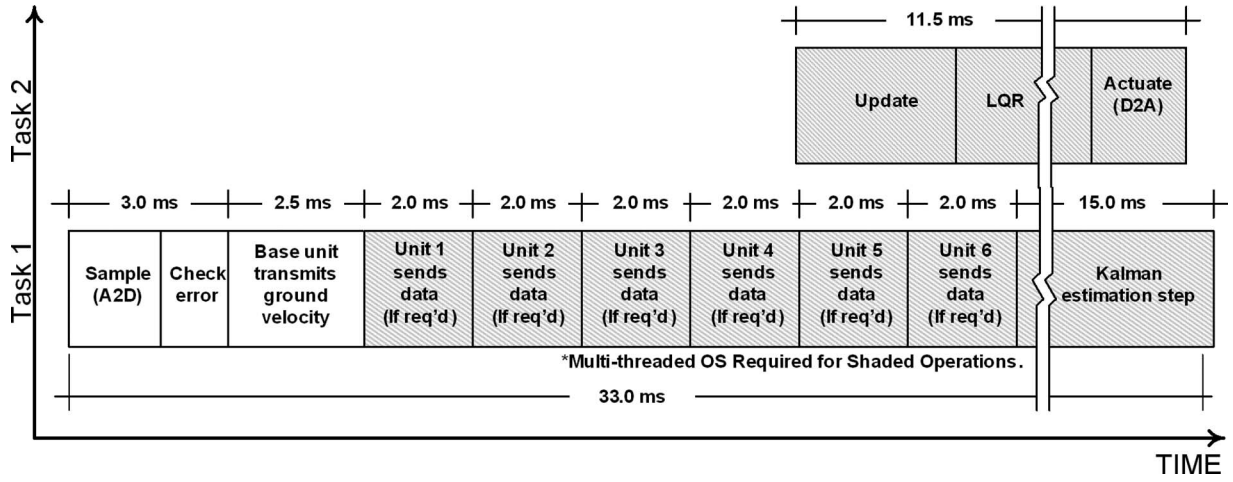

Fig. 3. Typical wireless sensor operation during each time step of discrete-time control system

weak direction. Steel floor plates are 2 cm thick and are supported on four sides by 0.5 cm thick L-section beams with equal 5 cm legs. The floor plates are connected to the beams by means of welded connections while the beams are connected to the columns via bolted connections. Wide flange $H100\times100\times6\times8$ steel section V braces are provided as the connection points for the MR dampers (Fig. 5) installed on every floor of the structure. The damping coefficient of the MR dampers varies with input current. As the current changes, the resulting magnetic field aligns ferrous particles suspended in a viscous fluid within the damper. A stronger magnetic field results in stronger particle alignment yielding higher damping ratios. The hysteretic, bilinear, biviscous MR damper model employed in this study was developed by Lin et al. (2005). The MR damper employed (Lord Corp. RD-1005-3) saturates at ±2.0 kN, has a 20 mm stroke, an input range of 0–2 A, and is powered by an independent 24 V power supply.

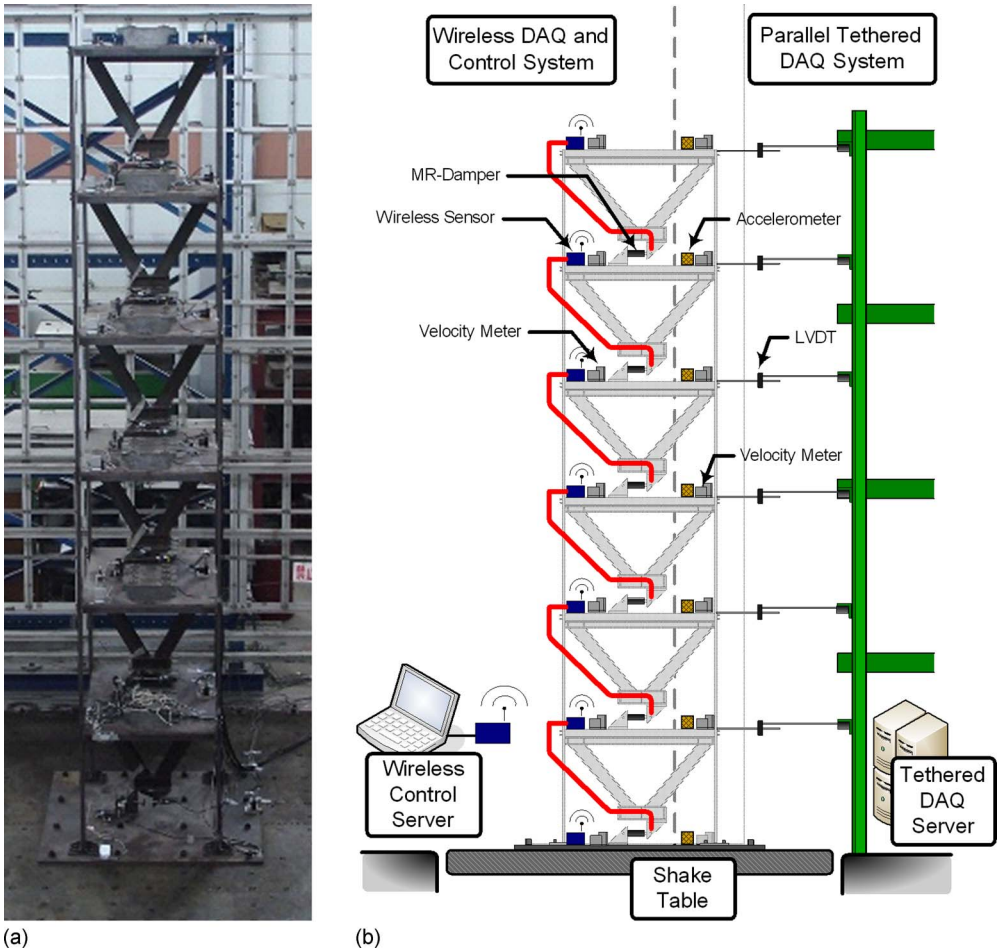

Fig. 4. Test structure for validation of wireless control system: (a) structure mounted to shake table; (b) instrumentation strategy

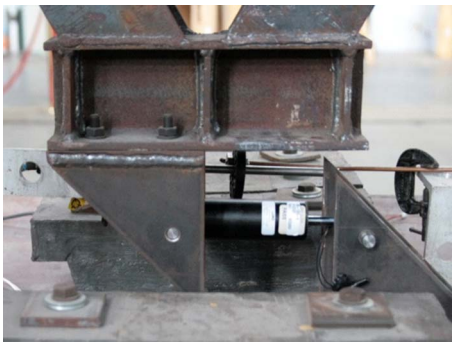

Fig. 5. MR damper (Courtesy of K.-C. Lu)

Each actuator has an associated Narada wireless sensor; the wireless sensor measures the lateral response of the structure using Tokyo Sokushin VSE-15D velocity meters. The VSE-15 has a sensitivity constant of 10 V/(m/s) and voltage output between ± 10 V. Its maximum measurable velocity is 1 m/s within a 0.1–70 Hz frequency band. A signal conditioning circuit shifts the mean from 0 to 2.5 V and deamplifies the sensitivity by a factor of four such that the velocity meters output is within the input range (0–5 V) of the wireless sensor's ADC. An additional wireless sensor is located on the table to measure and broadcast the reference (ground) motion to the network. Wireless sensors are used to calculate control forces and to command the MR dampers with voltage outputs ranging from 0 to 0.8 V. The aforementioned bilinear, biviscous model is used to convert the desired control force into an appropriate command voltage (Lynch et al. 2008). Desired control forces, with few and minor exceptions, are in the direction opposing motion. For any desired control force not opposing motion (which the MR damper cannot supply) the voltage output is set to 0 V (corresponding to minimum damping). The command voltage output by the sensor is converted by the damper power supply into a proportional amperage that falls within the operating range of the MR damper. Transmissions of state data occur only when the estimated state errors exceed the preset threshold.

The command to begin testing is sent from a personal computer (PC) via a Chipcon CC2420DBK development board connected through the PC's serial port. No further communication with the PC occurs until the test is over, at which time the wireless sensors transmit data back to the PC for offline analysis. The velocity response of the structure (relative to base), estimated velocity, and desired control force values recorded by the wireless sensors are reported back to the PC. Redundant cable based sensors record the displacement (Temposonics II position sensors) and velocity (Tokyo Sokushin VSE-15-AM) of the structure. Refer to Fig. 4(b) for a full schematic of the structure with the wireless and wired data acquisition systems detailed. The configuration of the MR dampers, unfortunately, do not allow for the use of load cells at the present time.

Control Performance Evaluation

As the state recovery error threshold is varied, control performance changes. Eight cost functions, J_1–J_8, through are used to characterize the controller performance as a function of error threshold. The first six cost functions, adapted from Ohtori et al. (2004), characterize the ability of controllers to reduce seismic responses important to design: interstory drift, floor acceleration, and base shear all normalized to the uncontrolled structural response due to the same ground excitation signal. Interstory drift minimization is important to reduce the likelihood of damage to the building system, especially to nonstructural elements such as windows, doors, and partitions. Floor acceleration is related to the force exerted on the structure and its occupants during a seismic event. Base shear is an important design parameter in sizing columns and footings. A pair of cost functions measures each of these parameters; one cost function compares single point absolute maximum values, while another compares the vector norm response over the entire test period

$$J_1 = \frac{\max_{\text{Floor},t}(|\mathbf{d}_{\text{controlled}}|)}{\max_{\text{Floor},t}(|\mathbf{d}_{\text{uncontrolled}}|)} \tag{21}$$

where $\mathbf{d} \in \mathbf{R}^{n\times N}$=interstory drift (where N=total number of time steps)

$$J_2 = \frac{\text{norm}(|\mathbf{d}_{\text{controlled}}|)}{\text{norm}(|\mathbf{d}_{\text{uncontrolled}}|)} \tag{22}$$

$$J_3 = \frac{\max_{\text{Floor},t}(|\ddot{\mathbf{x}}_{\text{controlled}}|)}{\max_{\text{Floor},t}(|\ddot{\mathbf{x}}_{\text{uncontrolled}}|)} \tag{23}$$

$$J_4 = \frac{\text{norm}(|\ddot{\mathbf{x}}_{\text{controlled}}|)}{\text{norm}(|\ddot{\mathbf{x}}_{\text{uncontrolled}}|)} \tag{24}$$

$$J_5 = \frac{\max(|\ddot{\mathbf{x}}_{\text{controlled}}\mathbf{W}|)}{\max(|\ddot{\mathbf{x}}_{\text{uncontrolled}}\mathbf{W}|)} \tag{25}$$

where $\mathbf{W} \in \mathbf{R}^{n\times 1}$=seismic mass vector. Finally

$$J_6 = \frac{\text{norm}(|\ddot{\mathbf{x}}_{\text{controlled}}\mathbf{W}|)}{\text{norm}(|\ddot{\mathbf{x}}_{\text{uncontrolled}}\mathbf{W}|)} \tag{26}$$

J_7 characterizes the average strain and kinetic energies in the system during the earthquake. Clearly, J_7 should be minimized to reduce the undesirable response energy of the system due to seismic excitation

$$J_7 = \frac{\left[\frac{1}{N}\sum_{i=1}^{N}\mathbf{z}_i^T\begin{bmatrix}\mathbf{K} & \mathbf{0}\\ \mathbf{0} & \mathbf{M}\end{bmatrix}\mathbf{z}_i\right]_{\text{controlled}}}{\left[\frac{1}{N}\sum_{i=1}^{N}\mathbf{z}_i^T\begin{bmatrix}\mathbf{K} & \mathbf{0}\\ \mathbf{0} & \mathbf{M}\end{bmatrix}\mathbf{z}_i\right]_{\text{uncontrolled}}} \tag{27}$$

The wireless bandwidth utilized by the wireless control system is characterized in J_8, which is the total number of data transmissions during the time of the ground motion divided by the total possible number of transmissions per sensor (N) times the total number of sensors (n)

$$J_8 = \frac{(\#\text{ Data Transmissions Sent})}{N \times n} \tag{28}$$

For centralized control, J_8 would be 1 while for fully decentralized control, J_8 would be 0; a number between 0 and 1 is an indirect measurement of where the partially decentralized control system falls on the spectrum between centralized and decentralized. These cost functions form the basis for comparing simulation and experimental results over a range of error threshold levels.

Simulation

To demonstrate the proposed control method, a numerical simulation is preformed in MATLAB using a model based on the six-story test structure. Specifically, the structure is modeled as a lumped-mass building with the mass of each floor equal to 862.85 kg. The identified stiffness for all stories is approximately 1.24 MN/m. The structure is lightly damped and is modeled using 0.5% Rayleigh damping. Wireless sensing units, assumed to be on each floor, record velocity measurements from collocated velocity meters while a seventh unit measures and broadcasts ground velocity to the network. Sensor noise is added to the signal in the form of Gaussian white noise with a standard deviation of 0.5 mm/s. The units compute the estimation error of the locally measured state data and compare it to the error threshold, retaining the estimate in cases where the error is below the threshold, otherwise replacing it with the measured value and transmitting that measured value to the rest of the network in cases where the error exceeds the threshold. Both perfect and lossy communications are simulated. For lossy communication, the chance of a dropped packet is modeled by use of a zero-mean, Gaussian random variable with unity standard deviation. A packet is considered to be "dropped" whenever the magnitude of the random variable exceeds an experimentally derived threshold. The magnitude of the random variable is multiplied by the number of neighboring units that choose to utilize the broadcast medium at the current step hence, the probability of a dropped packet increases when nearby units transmit and is zero when none of the neighboring units transmit.

Finally, the units calculate and apply the LQR control force and update the state estimate for the next time step. In the simulation, idealized skyhook actuators are assumed. To keep desired control forces below the limits of realistic semiactive actuators (e.g., MR dampers), the following values of $\mathbf{C_{LQR}}$ and $\mathbf{Q}_2$ are selected in the LQR formulation [Eq. (6)]

$$\mathbf{C_{LQR}} = \left[\begin{bmatrix} 1 & -1 & & 0 \\ 0 & 1 & \ddots & \\ \vdots & & \ddots & -1 \\ 0 & & & 1 \end{bmatrix} \quad 0.01 * \mathbf{I}\right], \quad \mathbf{Q_2} = 10^{-9}\mathbf{I} \tag{29}$$

The numerical simulation performs average Newmark integration of Eq. (1). The model is subjected to two different earthquake ground acceleration records: El Centro 1940 NS (USGS Station 117), Chi-Chi 1999 NS (TCU Station 076). The records are normalized to obtain absolute maximum accelerations of 1.0 m/s^2 (100 gal). The simulation is repeated with the error threshold of the state recovery algorithm altered. The velocity state values are compared at each degree of freedom with 25 error thresholds (that are logarithmically equally spaced between 0 and 5 m/s) applied in successive runs. Clearly, the 0 m/s threshold effectively triggers communications at each step resembling a centralized control system. Likewise, the 5 m/s threshold is so large that the threshold is never exceeded leading to a decentralized control system.

The ability of the controllers to reduce the seismic response of the structure changes as the error threshold varies. Maximum interstory drift as a function of floor is presented for a relevant set of error thresholds in Fig. 6 for the El Centro record (assuming perfect communication). In the simulation, the peak drift per floor increases monotonically with error threshold. The control performance, measured by error thresholds J_1–J_8, as a function of error

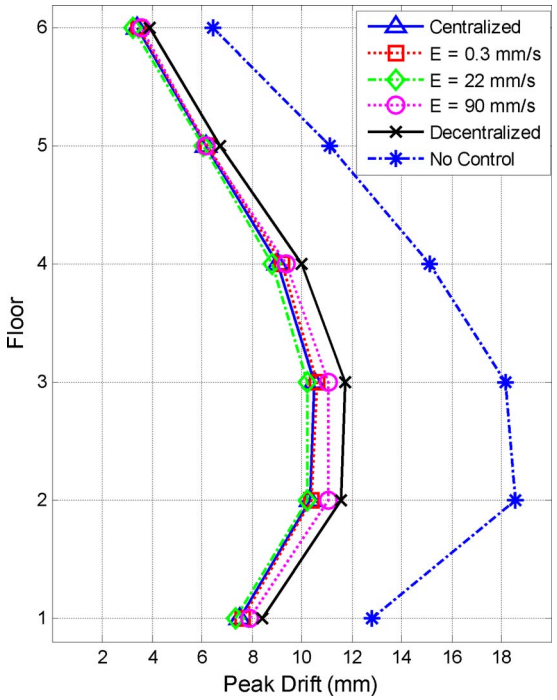

Fig. 6. El Centro (1.0 m/s^2) simulation results: peak interstory drift by floor

threshold is presented in Fig. 7 for both the perfect and lossy communication cases (El Centro and Chi-Chi). In the perfect communication case, performance generally transitions smoothly from centralized to fully decentralized control results as error threshold increases; the transition is characterized by a sigmoidal shaped function, as expected for J_1–J_7. However, in the case of lossy transmission, as bandwidth utilization decreases (as seen by J_8), the control performance generally improves slightly since fewer data packets are lost to collisions common in a centralized control system. This effect causes the error functions to actually go down as error threshold is initially increased. Eventually however, the error threshold becomes so large that the overall control performance degrades due to estimation error and performance begins to approach that of the fully decentralized case. In that case, the error threshold function rises with cost function values identical to the perfect communication case. These plots suggest an optimal error threshold level for performance in the case of lossy communications where enough data are transmitted to improve performance, but not too much to cause excessive packet collisions. For El Centro, this optimal error threshold is at 10 mm/s, while for the Chi-Chi earthquake, it is from 1 to 10 mm/s.

Experimental Results

Uniaxial lateral excitation is applied to the test structure by the shaking table corresponding to the ground motion record for El Cento and Chi-Chi normalized to 1.0 m/s^2 (100 gal) peak acceleration. Narada wireless sensing units operate autonomously to run the control network once the test has begun and interact with a PC server only at the end of a test to report data. The measurement performance of the Narada wireless sensor is presented in Fig. 8 with the wirelessly measured velocity comparing well to that of the wired system. In 1 day of testing, a ground motion record is repeated over an approximately logarithmically distrib-

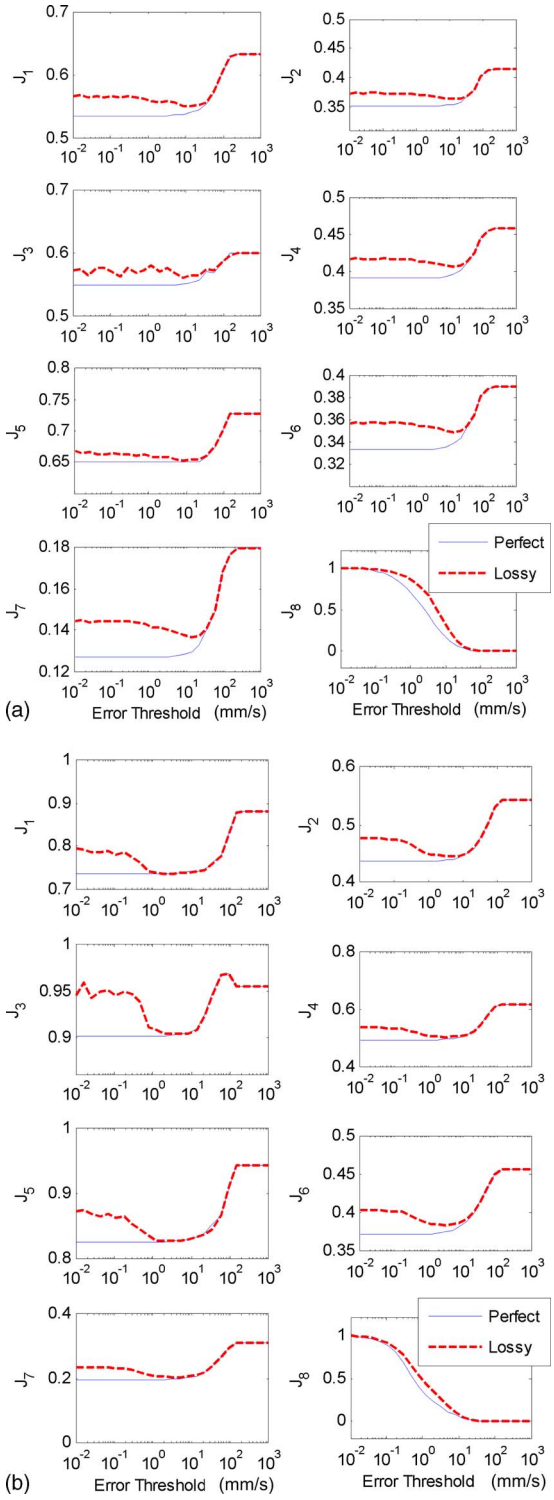

Fig. 7. Simulation results: (a) El Centro (1.0 m/s^2) cost functions; (b) Chi-Chi (1.0 m/s^2) cost

uted error threshold domain. As shown in Table 2, in total, 17 independent tests are conducted with increasing error thresholds. The 0 m/s threshold corresponds to a centralized case because at each time step, the threshold is exceeded forcing every sensor to communicate. Tests 2–16 increase the error threshold so as to render the system increasingly more decentralized. Test 17 is completely decentralized since the error threshold is so high, it is never exceeded.

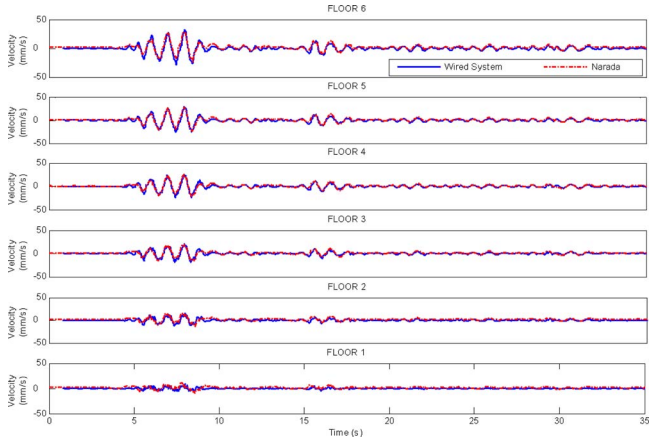

Fig. 8. Narada measured velocity output of test structure excited by El Centro (1.0 m/s^2) with cabled system response overlaid for comparison

Fig. 9 depicts the experimentally derived maximum drift response by floor for the El Centro record. Evident in the peak drift plots is the effectiveness of the wireless control system. The greatest peak drifts are witnessed for the structure without dampers installed. With the MR dampers installed but placed in a passive state (minimum and maximum damping settings), reduction in the interstory drifts are observed. However, the best performance occurs when the dampers are operated by the wireless control system. In general, as the error threshold is lowered, the redundant estimator framework yields better performance with respect to the peak interstory drift profile of the structure. This fact is more apparent when considering the cost functions J_1–J_8 that are presented in Fig. 10 for both the El Centro and Chi-Chi earthquake records (the El Centro results are an average of the 2 days of testing). The experimental results observed for both ground motion records are consistent with those obtained in simulation (Fig. 7). It should be noted that, due to time constraints during testing, J_8 was not logged for the Chi-Chi record. The majority of the cost functions initially decline as the error thresh-

Table 2. State Recovery Error Thresholds Experimentally Tested

Test number	Velocity error (m/s)
1	0 (centralized)
2	0.00002
3	0.00005
4	0.00008
5	0.0002
6	0.0005
7	0.0008
8	0.002
9	0.005
10	0.008
11	0.02
12	0.05
13	0.08
14	0.2
15	0.5
16	0.8
17	5 (decentralized)

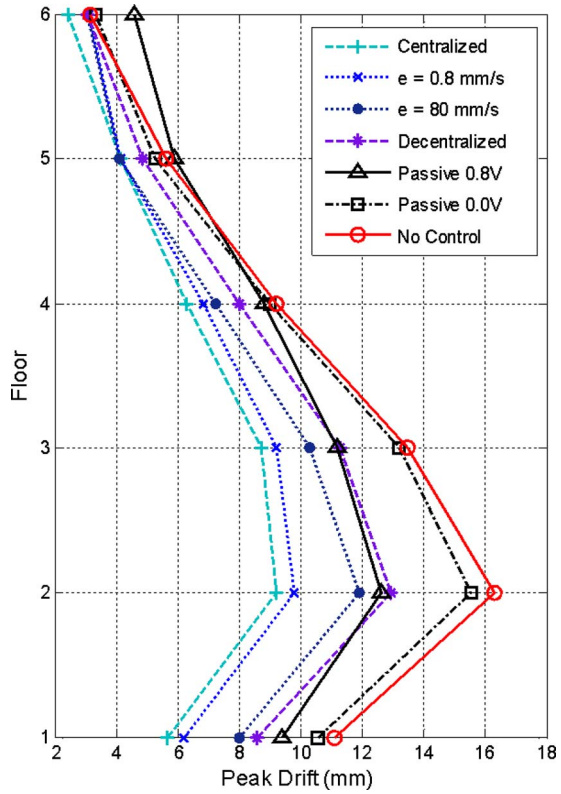

Fig. 9. El Centro (1.0 m/s^2) experimental results: peak interstory drift by floor

old is raised suggesting that the system performance improves initially because partial decentralization results in less data loss in the wireless channel (despite the TDMA communications). While initial gains are derived by alleviating the demand for the wireless channel, such gains are eroded as the error threshold is raised further due to decentralization of the control system. As a result, the cost functions begin to increase until is plateaus at large threshold values (essentially, when it is decentralized). This result lends further credence to the view advanced in the simulation phase that there exists an optimum error threshold level for control performance. For both earthquake records, it is likely that the optimal threshold is from 1 to 10 mm/s.

Conclusions

Transmission of every raw data point within a wireless control system increases delay, degrading the control performance, and drastically reducing battery life of the wireless sensors. Strategic use of wireless bandwidth can help to overcome some of the limitations of wireless control. An embedded estimator with embedded control force computation can be used for control in an actuator network whose size makes centralized control impractical due to bandwidth limitations. Limitations on the performance of fully distributed control make some sharing of data between units attractive. By sharing the most critical measured data points, those most different from their corresponding estimated data points, limited bandwidth can be utilized in an efficient manner. Furthermore, the performance of the controller varies from that of centralized control to that of distributed control as the error threshold is varied from low to high. Even for conservative communication models (e.g., TDMA) however, there appears to be

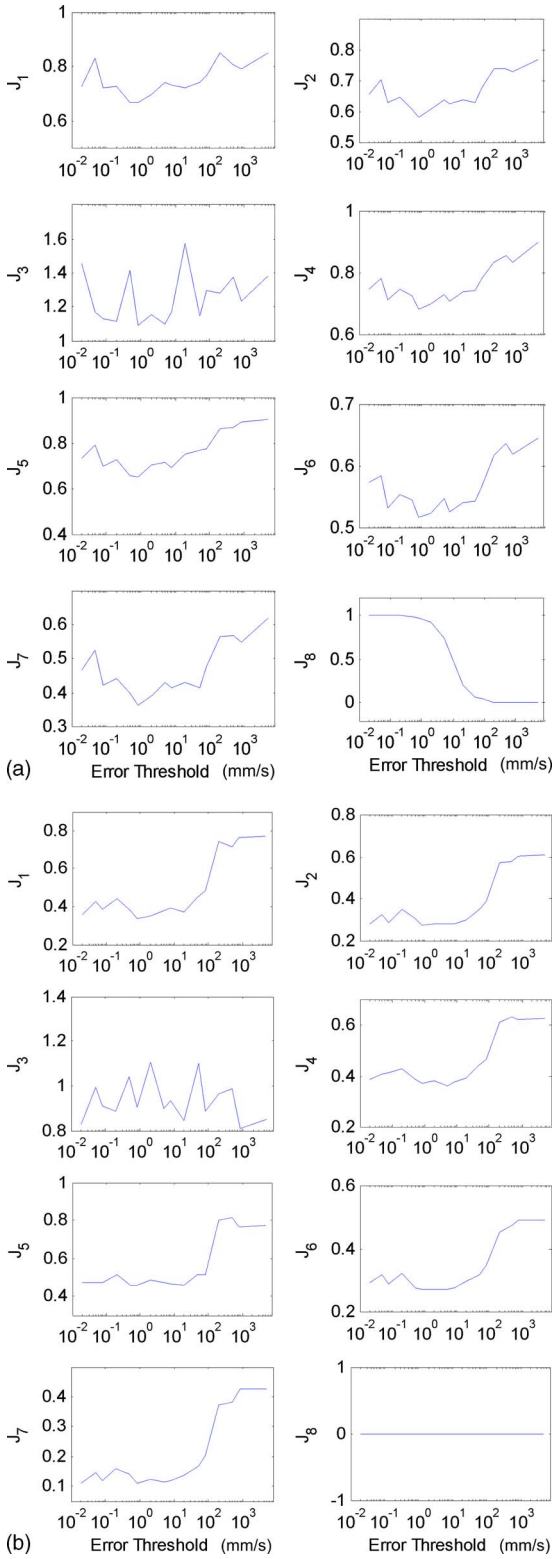

Fig. 10. Experimental results: (a) El Centro (1.0 m/s^2) cost functions; (b) Chi-Chi (1.0 m/s^2) cost

data loss resulting in a decline in performance for excessively low error threshold levels (suggesting an optimal threshold level between centralized and fully decentralized control). This effect may become more pronounced under less conservative communications models (e.g., CSMA-CA), a prospect that warrants further investigation. One might also wonder about the efficacy of the

base unit responsible for relaying ground motion data to the rest of the network as these data are critical for proper operation at any level of centralization. For this study, a larger time window is allocated to the base wireless sensor for communications, resulting in near perfect reception.

In this study, a so-called "optimal" threshold was determined experimentally, but an a priori means of establishing an error threshold would have more appeal. To identify the optimal threshold, first characterization of the behavior of the wireless system is necessary (e.g., packet collisions, drop rates, range issues, etc.) along with an analytical model of the transmission success rate as a function of utilized bandwidth. Second, an analytical model of the system performance as error accumulates (with a realistic estimation of sensor noise and disturbances) is necessary so that an acceptable level of control performance that is achievable by the wireless system can be identified. Further investigation is also warranted in control force derivation. It is implicit in the LQR approach used in this study that the applied control force will be the exact desired control force to guarantee optimality. Also, all models used in the LQR derivation assume linearity of the system. These assumptions are often unrealistic for civil structures due to the large forces required and the complicated dynamics of semiactive actuators such as MR dampers. Additional investigation is also warranted in error handling algorithms within the communications protocol derived for this study. Additionally, an adaptive error threshold may yield better results than the static threshold and should be investigated. Finally, organizing sensors into hierarchal clusters may reduce bandwidth usage, allow multichannel utilization, and improve data flow in large control systems.

Acknowledgments

The writers would like to acknowledge their gratitude for invaluable assistance provided by Professor Dawn Tilbury of the University of Michigan, Professor Kincho H. Law of Stanford University, Professor Yang Wang of the Georgia Institute of Technology, and Professor Chin-Hsiung Loh of National Taiwan University. This research has been sponsored by the Office of Naval Research Young Investigator Program (ONR YIP).

References

Arms, S. W., Townsend, C. P., Churchill, D. L., Hamel, M. J., Galbreath, J. H., and Mundell, S. W. (2004). "Frequency-agile wireless sensor networks." *Proc. SPIE*, 5389, 468–475.

Bryson, A. E., and Ho, Y. C. (1975). *Applied optimal control: Optimization, estimation, and control*, Hemisphere, New York.

Chintalapudi, K., Johnson, E. A., and Govindan, R. (2005). "Structural damage detection using wireless sensor-actuator networks." *Proc., 13th Mediterranean Conf. on Control and Automation*, Limassol, Cyprus, IEEE, Piscataway, N.J., 322–327.

Chu, S. Y., Soong, T. T., and Reinhorn, A. M. (2005). *Active, hybrid, and semi-active structural control: A design and implementation handbook*, Wiley, New York.

Clayton, E. H., Lu, C., Koh, B.-H., Xing, G., and Fok, C.-L. (2005). "Damage detection and correlation-based localization using wireless mote sensors." *Proc., 20th IEEE Int. Symp. on Intelligent Control, ISIC '05 and 13th Mediterranean Conf. on Control and Automation, MED '05*, Limassol, Cyprus, IEEE, Piscataway, N.J., 304–309.

Colandairaj, J., Irwin, G. W., and Scanlon, W. G. (2007). "Wireless networked control systems with QoS-based sampling." *IET Control Theory Appl.*, 1(1), 430–438.

Dyke, S. J., Spencer, B. F., Jr., and Sain, M. K. (1998). "An experimental study of MR dampers for seismic protection." *Smart Mater. Struct.*, 7(1), 693–703.

Franklin, G. F., Powell, J. D., and Emami-Naeini, A. (2002). *Feedback control of dynamic systems*, Prentice-Hall, Upper Saddle River, N.J.

Gavin, H., Hoagg, J., and Dobossy, M. (2001). "Optimal design of MR dampers." *Proc., U.S.–Japan Workshop on Smart Structures for Improved Seismic Performance in Urban Regions*, Seattle, 225–236.

Hatada, T., Kobori, T., Ishida, M., and Niwa, N. (2000). "Dynamic analysis of structures with Maxwell model." *Earthquake Eng. Struct. Dyn.*, 29(2), 159–176.

Hou, T.-C., Lynch, J. P., and Parra-Montesinos, G. (2005). "Local-based damage detection of cyclically loaded bridge piers using wireless sensing units." *Proc. SPIE*, 5768, 85–96.

Housner, G. W., et al. (1997). "Structural control: Past, present, and future." *J. Eng. Mech.*, 123(9), 897–971.

Kajima-Corporation. (2006). "Advanced structural control technologies, HiDAX: High damping system in the next generation." *Technical Pamphlet 06-134E*, Tokyo.

Kawka, P. A., and Alleyne, A. G. (2004). "Stability and feedback control of wireless networked systems." *Proc., 2005 American Control Conf.*, Portland, Ore., IEEE, Piscataway, N.J., 2953–2959.

Kurata, N., Kobori, T., Takahashi, M., Niwa, N., and Midorikawa, H. (1999). "Actual seismic response controlled building with semi-active damper system." *Earthquake Eng. Struct. Dyn.*, 28(11), 1427–1447.

Kurata, N., Spencer, B. F., Jr., and Ruiz-Sandoval, M. (2005). "Risk monitoring of buildings with wireless sensor networks." *Struct. Control Health Monit.*, 12(3), 315–327.

Kurino, H., Tagami, J., Shimizu, K., and Kobori, T. (2003). "Switching oil damper with built-in controller for structural control." *J. Struct. Eng.*, 129(7), 895–904.

Lin, L., Dyke, S., and Veto, R. (2007). "Wireless sensing and control of structural vibration from earthquake." *Proc., 26th Chinese Control Conf.*, Zhangjiajie, Hunan, China, IEEE, Piscataway, N.J., 194–198.

Lin, P.-Y., Roschke, P. N., and Loh, C.-H. (2005). "System identification and real application of a smart magneto-rheological damper." *Proc., 2005 Int. Symp. on Intelligent Control*, Limassol, Cyprus, IEEE, Piscataway, N.J.

Liu, X., and Goldsmith, A., (2004). "Wireless medium access control in networked control systems." *Proc., of 2004 American Controls Conf.*, Boston, IEEE, Piscataway, N.J.

Loh, C.-H., et al. (2007). "Experimental verification of a wireless sensing and control system for structural control using MR dampers." *Earthquake Eng. Struct. Dyn.*, 36(10), 1303–1328.

Lynch, J. P., et al. (2003). "Field validation of a wireless structural monitoring system on the Alamosa Canyon Bridge." *Proc. SPIE* 5057, 267–278.

Lynch, J. P., et al. (2004a). "Design and performance validation of a wireless sensing unit for structural monitoring applications." *Struct. Eng. Mech.*, 17(3), 393–408.

Lynch, J. P., and Loh, K. J. (2006). "A summary review of wireless sensors and sensor networks for structural health monitoring." *Shock Vib. Dig.*, 38(2), 91–128.

Lynch, J. P., Sundararajan, A., Law, K. H., Kiremidjian, A. S., and Carryer, E., (2004b). "Embedding damage detection algorithms in a wireless sensing unit for attainment of operational power efficiency." *Smart Mater. Struct.*, 13(4), 800–810.

Lynch, J. P., Wang, Y., Loh, K., Yi, J., and Yun, C.-B. (2006). "Performance monitoring of the Geumdang Bridge using a dense network of high-resolution wireless sensors." *Smart Mater. Struct.*, 15(6), 1561–1575.

Lynch, J. P., Wang, Y., Swartz, R. A., Lu, K.-C., and Loh, C.-H. (2008). "Implementation of a closed-loop structural control system using wireless sensor networks." *Struct. Control Health Monit.*, 518–539.

McMahon, S., and Makris, N. (1997). "Large-scale ER-damper for seismic protection." *Proc. SPIE* 3045, 140–147.

Nagarajaiah, S., and Mate, D. (1998). "Semi-active control of continu-

ously variable stiffness system." *Proc., 2nd World Conf. of Structural Control*, New York, IEEE, Piscataway, N.J., 397–405.

Nagayama, T., Spencer, B. F. Jr., and Rice, J. A. (2007). "Structural health monitoring utilizing Intel's Imote2 wireless sensor platform." *Proc. SPIE*, 6529(2), 6592943.

Ohtori, Y., Christenson, R. E., and Spencer, B. F., Jr. (2004). "Benchmark control problems for seismically excited nonlinear buildings." *J. Eng. Mech.*, 130(4), 366–385.

Pakzad, S. N., Fenves, G. L., Kim, S., and Culler, D. E. (2008). "Design and implementation of scalable wireless sensor network for structural monitoring." *J. Infrastruct. Syst.*, 14(1), 89–101.

Ploplys, N. J., Kawka, P. A., and Alleyne, A. G. (2004). "Closed-loop control over wireless networks." *IEEE Control Syst. Mag.*, 24(3), 58–71.

Soong, T. T. (1990). *Active structural control: Theory and practice*, Longman Scientific and Technical, Essex, U.K.

Spencer, B. F., and Nagarajaiah, S. (2003). "State of the art of structural control." *J. Struct. Eng.*, 129(7), 845–856.

Stengle, R. F. (1994). *Optimal control and estimation*, Dover, Mineola, N.Y.

Straser, E., and Kiremidjian, A. S. (1998). "Modular, wireless damage monitoring system for structures." *Rep. No. 128*, John A. Blume Earthquake Engineering Center, Stanford, Calif.

Swartz, A., Jung, D., Lynch, J. P., Wang, Y., Shi, D., and Flynn, M. P. (2005). "Design of a wireless sensor for scalable distributed in-network computation in a structural health monitoring system." *Proc., 5th Int. Workshop on Structural Health Monitoring*, Stanford, Calif.

Tanner, N. A., Farrar, C. R., and Sohn, H. (2002). "Structural health monitoring using wireless sensing system with embedded processing." *Proc. SPIE*, 4704, 215–224.

Wang, Y., Swartz, R. A., Lynch, J. P., Law, K. H., Lu, K.-C., and Loh, C.-H. (2006a). "Decentralized civil structural control using a real-time wireless sensing and control system." *Proc. 4th World Conf. on Structural Control and Monitoring (4WCSCM)*, San Diego.

Wang, Y., Swartz, R. A., Lynch, J. P., Law, K. H., Lu, K.-C., and Loh, C.-H. (2006b). "Wireless feedback structural control with embedded computing." *Proc., SPIE—Health Monitoring and Smart Nondestructive Evaluation of Structural and Biological Systems V*, San Diego, v. 6177, SPIE, 61770C-1-12.

Whelan, M. J., Gangone, M. V., Janoyan, K. D., Cross, K., and Jha, R. (2007). "Reliable high-rate bridge monitoring using dense wireless sensor arrays." *Proc., Int. Workshop on Structural Health Monitoring*, Stanford, Calif.

Yook, J. K., Tilbury, D. M., and Soparkar, N. R. (2002). "Trading computation for bandwidth: Reducing communication in distributed control systems using state estimators." *IEEE Trans. Control Syst. Technol.*, 10(4), 503–518.

Zimmerman, A. T., Shiraishi, M., Swartz, R. A., and Lynch, J. P. (2008). "Automated modal parameter estimation by parallel processing within wireless monitoring systems." *J. Infrastruct. Syst.*, 14(1), 102–113.